ASSOCIAZIONE NAZIONALE ITALIANA DI INGEGNERIA SISMICA ANIDIS
Italian National Association of Earthquake Engineering

XVIII CONVEGNO ANIDIS
L'ingegneria sismica in Italia
ASCOLI PICENO 2019
15-19 Settembre

Macroelement modelling of a monitored URM school building accounting for seismic damage accumulation

Francesco Graziotti[a], Marco Solenghi[a], Gabriele Guerrini[a], Andrea Penna[a]
[a] *Department of Civil Engineering and Architecture (DICAr), University of Pavia, via Ferrata 3, 27100 Pavia, Italy*

Keywords:Unreinforced masonry (URM), Seismic sequence, Numerical Modelling, Dynamic Analysis, Damage accumulation, Instrumented structure

ABSTRACT
The Italian Structural Seismic Observatory (OSS), a network of permanent sensors mainly installed in public buildings by the Department of Civil Protection, monitored the elementary school of the town of Visso, a 4800-cubic-metre, two-storey stone masonry building, during the seismic sequence that stroke central Italy in 2016. Twenty-three accelerometric channels allowed recording the dynamic response of the building during the entire sequence, which caused the collapse of portions of masonry walls and of floor diaphragms. Building surveys after the major events allowed tracking the damage evolution through the entire sequence. A detailed geometrical and mechanical characterization campaign of the structural system, performed before the sequence, complemented the data provided by the OSS, allowing the development of a reliable equivalent-frame numerical model of the building, implemented in the software TREMURI. The comparison between data recorded on site and nonlinear time-history analysis results gave the opportunity to verify with an actual case some modelling assumptions, typically validated against smaller shake-table experiments, especially concerning damage accumulation and effects of major plan irregularity.

1 INTRODUCTION

Post-earthquake surveys of buildings subjected to ground shaking constitute an essential source of information to qualitatively study the seismic vulnerability of existing structures (e.g. Akansel et al. 2014), but do not provide quantitative information about their the dynamic response.

On the other hand, dynamic shaking table tests on full-scale models represent the most complete laboratory experiments to investigate the seismic behavior of structures and components, especially in the non-linear range (e.g. Magenes et al. 2014, Beyer et al. 2015, Kallioras et al. 2018). The main limitations of this type of tests are essentially three: (i) the limited dimensions of the specimens due to shaking table constraints, (ii) the difficulty to account for soil-structure interaction, and (iii) the impossibility to test structures in their actual conditions (e.g. complete detailing, aging effects, non-structural components).

In-situ measurements on actual instrumented structures excited by earthquakes represent an important complementary source of information, because they allow overcoming the limitations associated with qualitative in-situ observations and shaking table tests. However, the depth of information and knowledge about the structure, which is normally associated with laboratory tests, cannot be easily acquired in the field. Currently, literature lacks information about instrumented structures hit and heavily damaged by seismic events.

In this framework, a large amount of valuable data has been provided by the Italian Structural Seismic Observatory (OSS) since the 1990s. This is a network of permanent seismic monitoring systems belonging to the Department of Civil Protection (DPC), installed mostly on public buildings, on some bridges, and on a few dams (Dolce et al. 2017).

The elementary school of the town of Visso (MC, Italy), a 4800-cubic-metre, two-storey stone masonry building was one of this monitored building. Twenty-three accelerometric channels allowed recording the dynamic response of the building during the entire sequence, which caused the collapse of portions of masonry walls and floor diaphragms.

This paper briefly describes the building in terms of geometrical and mechanical properties, the instrumentation layout, and the post-processing of the recorded data. The work then proposes a numerical simulation based on the equivalent-frame approach. The recorded seismic performance of the structure is compared with the numerical prediction, supporting the effectiveness of the equivalent-frame model (Lagomarsino et al. 2013, Penna et al. 2014) in capturing the nonlinear dynamic behaviour and damage accumulation throughout the seismic sequence.

2 DESCRIPTION OF THE BUILDING

The elementary school of Visso was built in the 1930s, with an unreinforced masonry (URM) structure that consists of undressed stone blocks with a regular bond. As described by Cattari et al. 2019, the overall volume of the building was about 4800 m^3, distributed over two stories above ground and a partial basement below wing "B" (Figure 1). Each floor area was about 600 m^2 with an irregular T-shape plan (Figure 1) composed by two rectangular portions: the main body, labelled as wing "A", oriented in NW-SE direction, and a smaller wing, indicated as wing "B", orthogonal and continuous with the first one.

2.1 Building features

A detailed geometric and mechanical characterization, commissioned by the Italian Department of Civil Protection in 2009, represents the main source of information about the building.

The vertical structure, extending for the entire height of the school, consisted of double-leaf masonry piers built with undressed stone blocks with variable thickness ranging from 67 to 85 cm at the first storey, and from 50 to 78 cm at the attic.

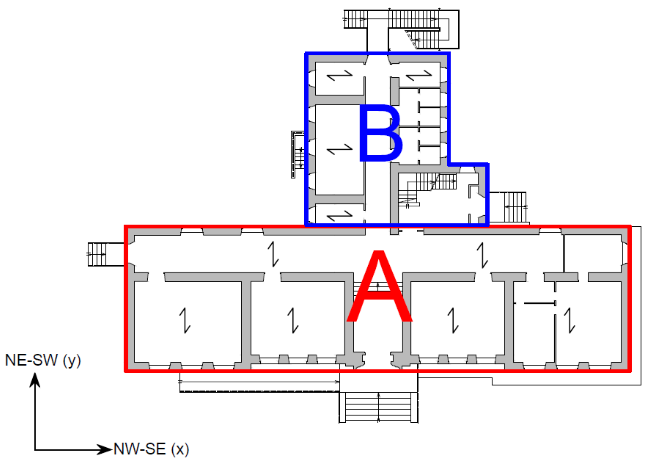

Figure 1. Ground floor plan view of the school.

Visual and video-endoscopic inspections, computed-tomography scans, and thermo-graphic surveys showed a regular texture of the masonry walls with transversal connection between the two leaves and among orthogonal walls. The characterization campaign included a double-flatjack test, from which the elastic modulus (E = 1733 MPa) was obtained. Furthermore, laboratory tests on samples and in-situ penetration tests on mortar proved a good quality of this material, with mean values of compressive strength ranging from 1.5 to 1.7 MPa.

The floor typologies and orientations were defined based on characterization tests that included video-endoscopic investigations and georadar surveys. The ground and the first floors consisted of one-way or two-way systems with reinforced concrete joists, hollow clay blocks, and a concrete topping slab; the attic floor was realized with steel joists, instead. The roof, built with a hipped composite timber-concrete structure, was surveyed by direct visual inspections.

Moreover, a retrofit following the M6.0 earthquake that stroke Central Italy in 1997 was reported, with several interventions: repair and consolidation by mortar injection of some internal load-bearing piers, addition of brick-masonry walls in the stairwell, reinforcement with steel profiles around large first-storey openings, out-of-plane strengthening of the perimeter walls with steel profiles, partial replacement of the composite roof structure, and addition of a connection system between roof and perimeter walls (Graziotti et al., 2019).

2.2 Instrumentation

The building was monitored by the Italian OSS. The monitoring system installed in the school consisted of 11 multiaxial accelerometers with sampling rate of 250 Hz. These sensors were organized as schematically shown in Figure 2: a tri-axial accelerometer (the Near Field sensor, labelled as "NF") was installed in close proximity of the foundations to record the input signal at the base of the building, while 10 bi-axial accelerometers were mounted at the first and second floors of the school to record the two horizontal components of the seismic response exhibited by different portions of the structure, for a total of 23 recording channels. The channels were connected to the digital acquisition unit that transmitted the acceleration signals acquired by the sensors to the server of the DPC.

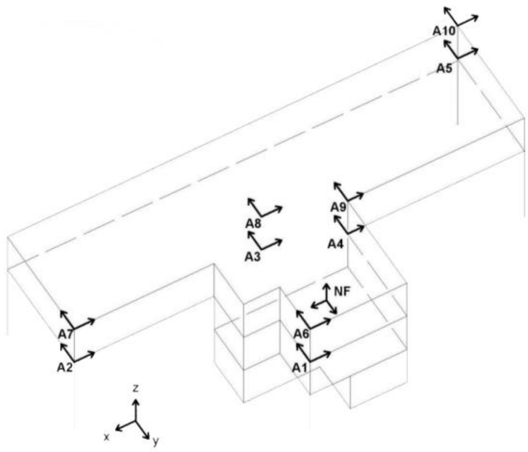

Figure 2. Monitoring system: sensor layout.

3 SEISMIC EVENTS

The database of the seismic events recorded by the monitoring system installed on the building is extremely large. In this work, in order to focus on the seismic damage accumulation, the more interesting subset listed in Table 1 was taken in consideration.

These records were taken from the most destructive events of the seismic sequence that stroke central Italy in August and October 2016, with magnitude exceeding 5.0 and epicentre at a close range from the town of Visso. The effects of these earthquakes on the masonry structure were also documented by several inspections, including one on June 27, 2017. The observed damage denoted the full development of shear mechanisms on piers and spandrels all over the structure, already activated during the first event occurred on August 24, 2016.

Table 1. Seismic events (from OSS database).

Signal ID	**Epicenter Location (Distance)**	**M**	**Date [UTC]**	**PGA NW-SE [g]**	**PGA NE-SW [g]**
SM1	Accumuli (28 km)	6.0	2016-08-24	0.334	0.322
SM2	Castel S.A. sul Nera (7 km)	5.4	2016-10-26	0.294	0.210
SM3	Ussita (4 km)	5.9	2016-10-26	0.363	0.476
SM4	Norcia (11 km)	6.5	2016-10-30	0.294	0.301

A higher damage concentration was observed in wing “B”, which exhibited a more flexible behaviour compared to wing “A”, causing the out-of-plane collapse of a corner and the collapse of significative parts of the floors (Figure 3). Starting from the signals recorded by the monitoring system, single and double integration of the acceleration time histories related to each accelerometer provided estimation of velocities, displacement and deformations throughout the entire seismic sequence.

4 NUMERICAL MODEL

The seismic response of the school during the earthquakes listed in Table 1 was simulated with nonlinear dynamic analyses on a three-dimensional model of the building (Figure 4) in the software TREMURI (Lagomarsino et al. 2013; Penna et al. 2014). The structure was discretized with the equivalent-frame approach, adopting the nonlinear macroelement implemented by Bracchi et al. (2018) to describe the in-plane cyclic response of each masonry structural member.

Figure 3. Damages in wing “B” after the seismic sequence: out of plane collapse of a corner (top), partial collapse of the attic floors (bottom).

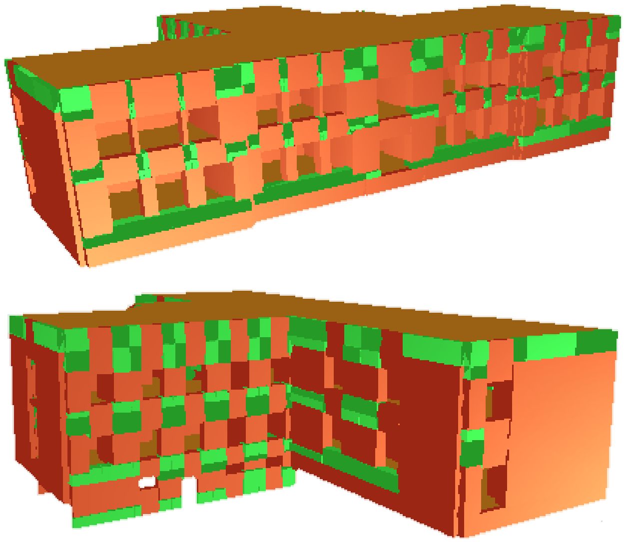

Figure 4. 3D views of the numerical model of the building developed within the research version of TREMURI.

The dynamic analyses were conducted in sequence, adopting as input the acceleration signals recorded by the NF accelerometer, and carrying over the cumulative damage of each element from previous runs, to represent the real initial conditions for each event. Furthermore, in order to simulate the variation of dissipative capacity caused by cumulative damage, the Rayleigh damping model described by Graziotti et al. (2019) was adapted to obtain damping ratios of 3.5% for SM1 and of 2% for all following events.

The mechanical proprieties adopted for the masonry elements are listed in Table 2. The compressive and tensile strength, f_c and f_t, were defined based on the Italian building code NTC2008 (MIT 2008; MIT 2009) while the elastic modulus E and the shear modulus G were slighly calibrated to better capture the dynamic behavior of the structure. Parameters Gc_t and β define the peak displacement and the softening branch of the masonry inelastic constitutive relationship, while μ_{eq} is used to assign an equivalent Mohr-Coulomb shear strength criterion to the spandrels.

The diaphragms were modelled as linear elastic orthotropic membranes with four or three nodes, characterized by thickness t, Young's moduli E_1 and E_2, and shear modulus G. Standard values were assigned to the mechanical proprieties, listed in Table 3, based on floor and roof typologies. In order to capture the higher deformability observed in the slab of building wing "B", the diaphragms of this wing were modelled with a secant elastic modulus in order to simulate the elasto-plastic response of the in-plane damaged floor.

Table 2. Masonry mechanical proprieties assumed in model. Material distinguished for Piers (P) and Spandrels (S).

ID	E [MPa]	G [MPa]	f_c [MPa]	f_t [MPa]	Gc_t [-]	β [-]	μ_{eq} [-]
P1	2600	867	3.20	0.10	2.5	0.5	-
P2	2700	900	5.20	0.18	2.5	0.5	-
P3	3899	1300	6.24	0.19	2.5	0.5	-
P5	2600	867	4.16	0.13	2.5	0.5	-
S4	2600	867	3.20	0.10	4.0	0.0	0.5
S6	2600	867	4.16	0.13	4.0	0.0	0.5

Table 3. Diaphragm mechanical proprieties assumed in model.

Floor	Portion	t [mm]	E_1 [MPa]	E_2 [MPa]	G [MPa]
Ground	A	60	30000	30000	13000
	B	60	46000	46000	12500
First	A	50	50400	50400	12500
	B*	50	2740	1630	680
Second	A	40	9150	0	12500
	B*	40	250	0	345
Roof	A	40	9150	0	12500
	B*	40	250	0	345

**modelled with secant stiffness based on the maximum deformation recorded*

For this scope, the slab in-plane shear strength V_{Rd} was approximately quantified following the specifications of ACI 318-14 (ACI, 2014) for concrete elements without shear reinforcement, assuming a compressive strength $f_c' = 20$ MPa, cross-sectional width $h = 6$ m, and thickness $t = 50$ mm (Figure 5):

$$V_{Rd} = 0.17\sqrt{f_c'} \cdot h \cdot t = 225 \text{ kN}. \qquad (1)$$

The reference shear deformation of the first-floor diaphragm was estimated from the maximum difference between the displacements at the locations of accelerometers A1 and A4 during event SM1, $\Delta u_{max} = 18$ mm. The secant shear modulus G^* was estimated inverting the elastic shear stiffness relationship for the cantilever beam configuration, with length $L = 13.60$ m and shear factor $\chi = 1.2$ (Figure 5):

$$G^* = \frac{V_{Rd}}{\Delta u_{max}} \cdot \frac{\chi \cdot L}{t \cdot h} = 680 \text{ MPa}. \qquad (2)$$

The secant shear modulus at the first floor was approximately equal to 5% of the initial elastic value assumed for the undamaged slab (12500 MPa). The elastic moduli E_1 and E_2 were then modified adopting the same reduction factor.

A similar operation was conducted on the attic and roof diaphragms, resulting in a secant stiffness equal to about 2.5% of the undamaged one at these locations.

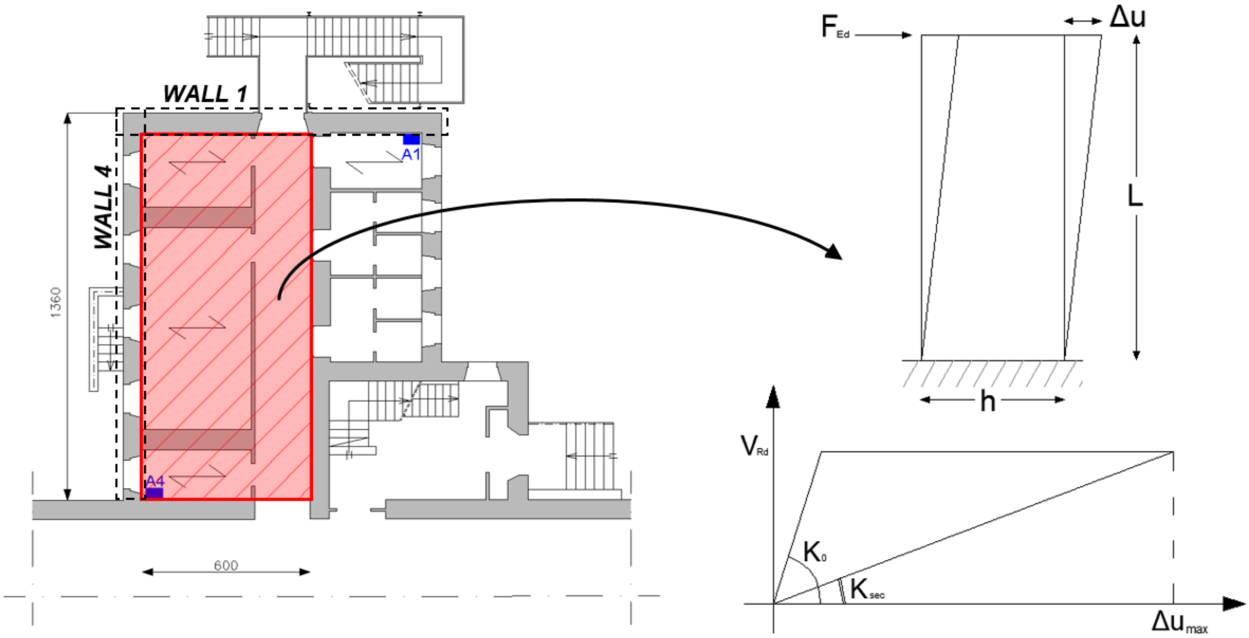

Figure 5. Simplified cantilever scheme for evaluating the secant stiffness of wing “B” diaphragms.

5 COMPARISON BETWEEN NUMERICAL AND RECORDED RESULTS

As a first result, Figure 6 compares the first-storey drift-ratio time-histories at the free edge of wing “B”, derived from accelerometer A1 (black) and from the numerical simulation on wall 1 (red) under SM1, adopting different elastic moduli for the diaphragms of wing “B”. For the location of accelerometer A1 see Figure 2, for that of wall 4 see Figure 5. The initial undamaged stiffness (Figure 6, top) led, in this case, to relevant errors on the estimate of the dynamic behaviour of this wing. On the other hand, the secant parameters estimated previously (Figure 6, bottom) allowed a more accurate prediction of the period and amplitude of the local dynamic response, with an error of about 8% on the maximum amplitude of the signal.

A comparison between recorded (black) and simulated (red) hysteretic curves, obtained plotting the base shear against the top floor displacement, is shown in Figure 7 for the 4 main events of the seismic sequence and for the two principal direction in the horizontal plane, NE-SW (or X) and NW-SE (or Y). During the seismic sequence, the school exhibited a response characterized by a high level of nonlinearity, as testified by the cumulative damage on masonry and floor structural elements.

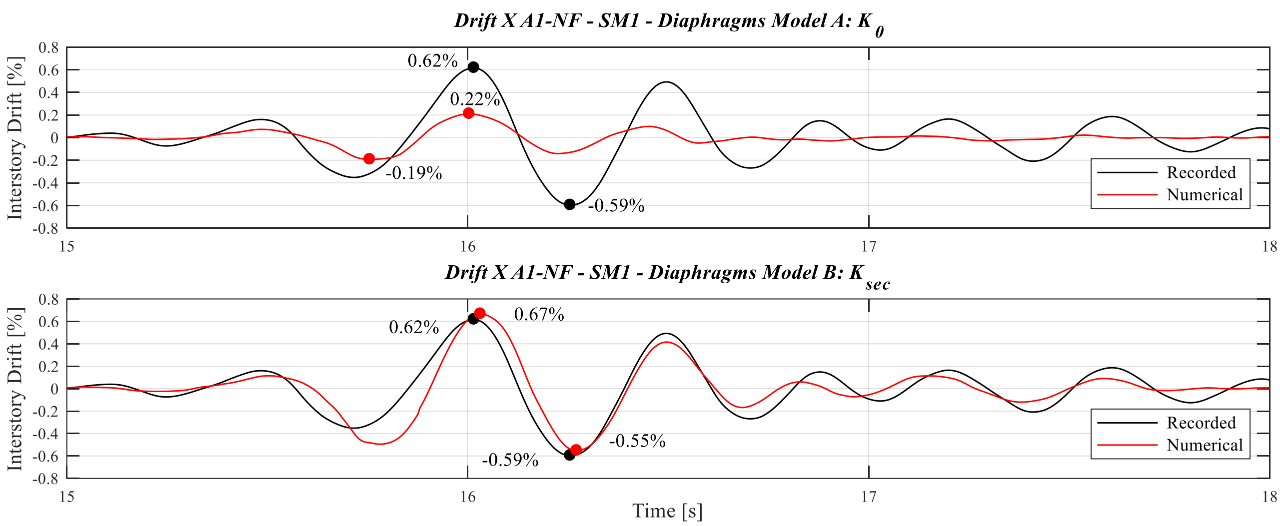

Figure 6. First-storey drift-ratio time-histories obtained from accelerometer A1 (black) and from numerical simulation on wall 1 (red) under SM1: initial undamaged stiffness (top) and secant stiffness (bottom) for wing “B” diaphragms.

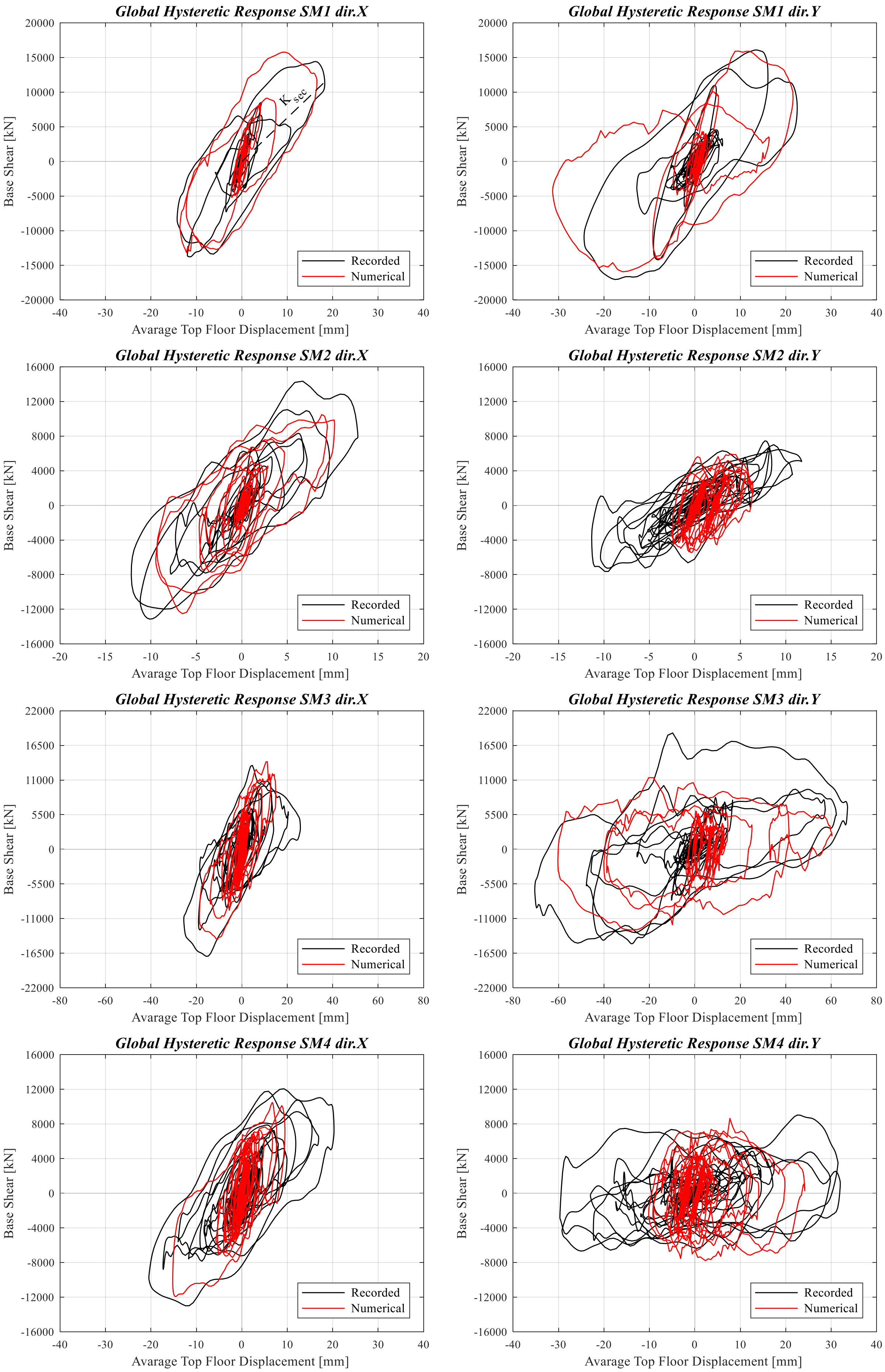

Figure 7. Global hysteretic response: X direction (left), Y direction (right). From top to bottom: SM1 (August 24, 2016), SM2 and SM3 (October 26, 2016), and SM4 (October 30, 2016).

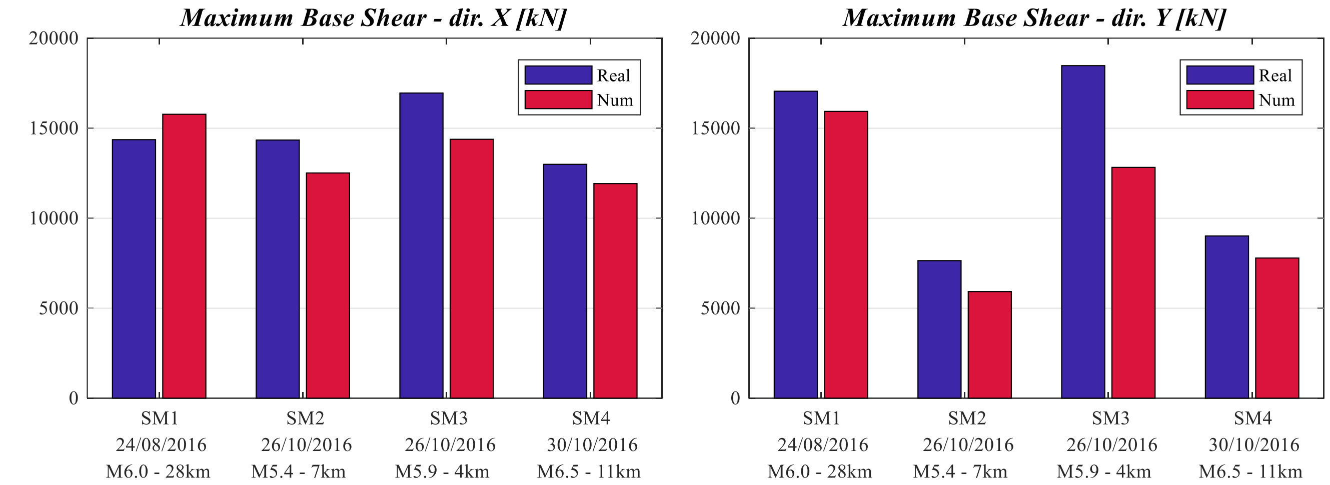

Figure 8. Maximum absolute base shear: actual recordings (blue) and numerical simulation (red).

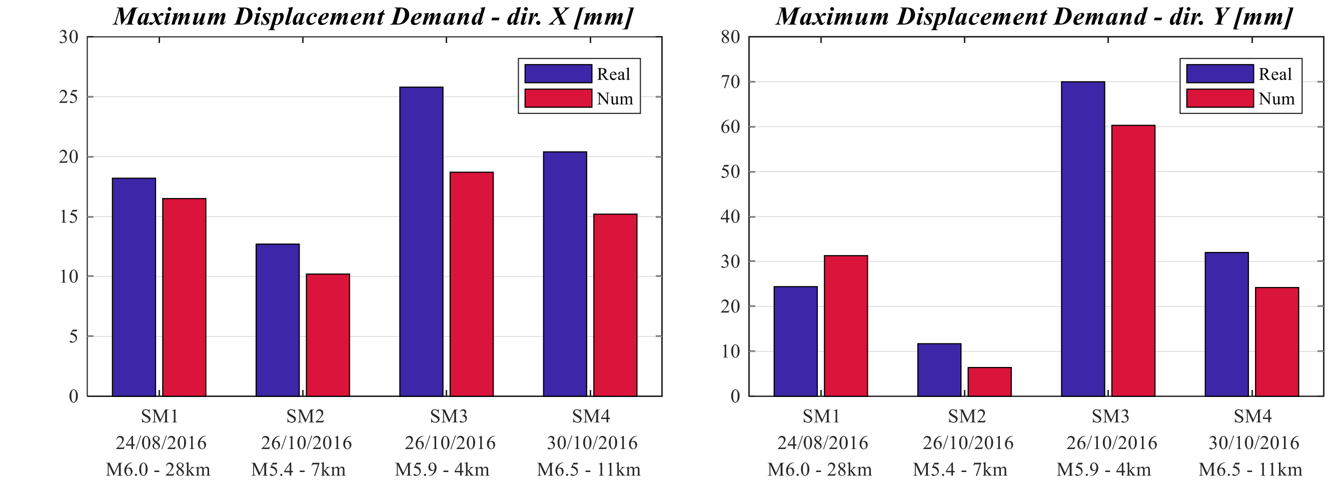

Figure 9. Maximum absolute average top displacement: actual recordings (blue) and numerical simulation (red).

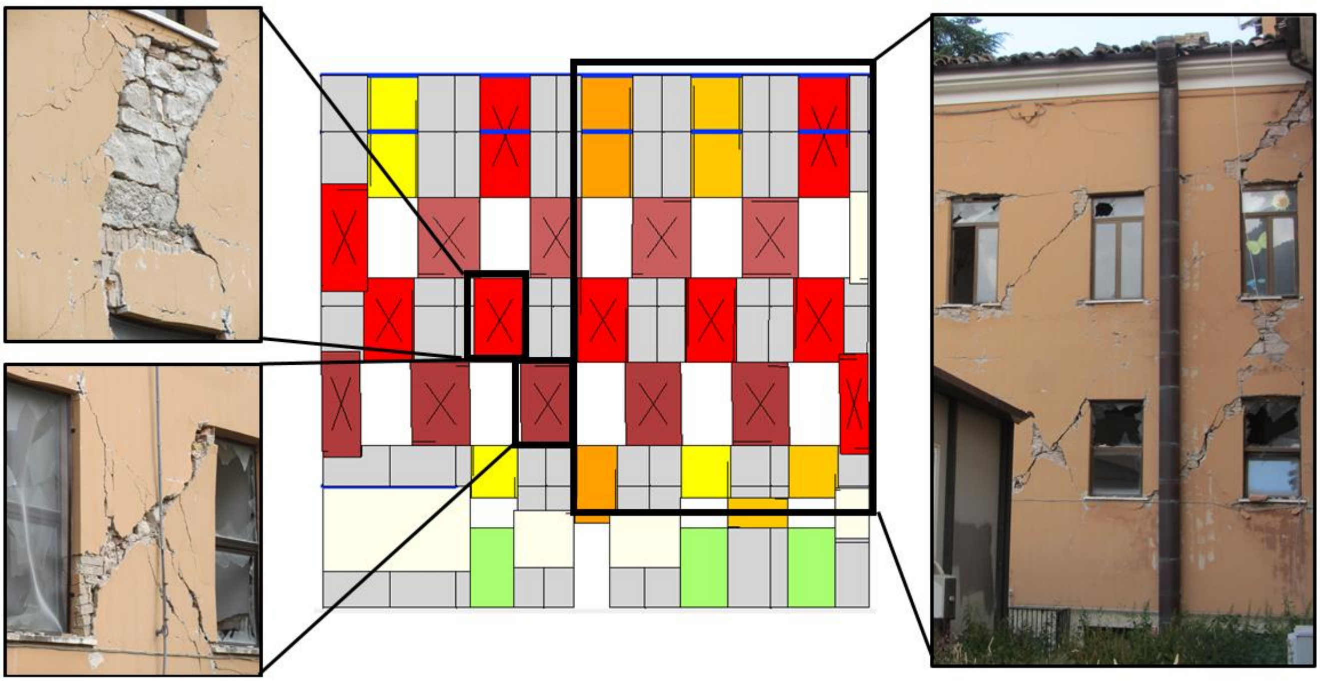

Figure 10. Comparison between the damage obtained from the numerical simulation and the one observed on the building at the end of the seismic sequence, wall 4 of wing "B".

The numerical model was able to simulate adequately the inelastic behaviour of the building in terms of global stiffness decay, amplitude of hysteretic cycles, maximum base shear (Figure 8), and average top displacement demand (Figure 9). A better accuracy was obtained during the first two events, especially in the X direction, where the structure responded with in-plane wall mechanisms that were well caught by the model. The increased approximation in the following events is probably due to the fact that, during SM3, a significant portion of wall 1 in wing "B" (Figure 5) developed an out-of-plane mechanism that was not explicitly modelled. Furthermore, comparing the accuracy of the model in the two horizontal directions, a slight underestimation of displacement demand in the weak Y direction can be observed.

Figure 10 compares the damage level observed at the end of the seismic sequence on wall 4 in wing "B" (Figure 5) with the one obtained by numerical analysis. The adopted discretization was able to simulate with good accuracy the development of shear mechanisms (graphically represented with a cross sign) on piers and spandrels as well as the entire masonry façade behaviour, demonstrating the validity of the equivalent-frame approach in capturing the seismic response of walls with regularly distributed openings which develop in-plane mechanisms.

6 CONCLUSIONS

This paper discussed the numerical simulation of the seismic response of a stone masonry school building, located in the town of Visso, Italy, instrumented with several accelerometers by the Italian Department of Civil Protection as part of the Structural Seismic Observatory.

The building was subjected to ground motions caused by the earthquake sequence that hit Central Italy starting on August 24, 2016. Double integration of the accelerometer signals allowed deriving displacements, which provided a full quantification of the nonlinear dynamic response of the building.

The numerical model was based on the equivalent-frame approach for masonry walls, with geometrical and material properties obtained from extensive in-situ surveys. It is worth noting that this macroelement requires a limited number of mechanical properties, which were easily estimated with in-situ non-destructive or semi-destructive characterization tests and integrated with standard values where necessary.

Moreover, damage accumulation in the masonry elements was explicitly accounted for within the model. This feature was essential for capturing the dynamic behaviour of the structure after the first event.

The floor slabs were characterized by finite stiffness and strength. Modelling their nonlinear behaviour through an equivalent linear approach with secant stiffness resulted to be necessary to capture the behaviour of this structure, especially in light of its irregular plan configuration.

Good accuracy was observed for the numerical prediction in terms of damage pattern, displacement histories, and global hysteretic response under all strong motions that caused extensive in-plane shear damage to the piers and spandrels of the building.

The results of this study demonstrate the validity of the equivalent-frame modelling approach for masonry buildings, especially when openings are regularly distributed on their walls and out-of-plane mechanisms do not dominate their seismic response. Moreover, they complement on a larger scale the findings of smaller laboratory shake-table tests conducted worldwide.

This study highlights the opportunity offered by the combination of geometric surveys, in-situ characterization tests, permanent monitoring, and numerical modelling to assess the seismic vulnerability of strategic structures and infrastructures, and to tailor retrofit intervention campaigns for an effective risk mitigation strategy.

ACKNOWLEDEGEMENTS

The results described in this document were achieved within the national research project ReLUIS-DPC 2017–2018 (www.reluis.it) supported by the Italian Civil Protection Agency.

REFERENCES

Akansel, V., Ameri, G., Askan, A., Caner, A., Erdil, B., Kale, Ö., Okuyucu, D., 2014. The 23 October 2011 MW7.0 Van (Eastern Turkey) Earthquake: Interpretations of Recorded Strong Ground Motions and Post-Earthquake Conditions of Nearby Structures. *Earthquake Spectra*, **30**(2), 657-682.

American Concrete Institute, 2014. *Building Code Requirements for Structural Concrete (ACI 318-14): Commentary on Building Code Requirements for Structural Concrete (ACI 318R-14): an ACI Report.* American Concrete Institute. ACI.

Beyer, K., Tondelli, M., Petry, S., Peloso, S., 2015. Dynamic testing of a four-storey building with reinforced concrete and unreinforced masonry walls: prediction, test results and data set. *Bulletin of Earthquake Engineering*, **13**(10), 3015-3064.

Bracchi, S., Galasco, A., Penna, A., Magenes, G., 2018. An improved macroelement model for the nonlinear analysis of masonry buildings. *10th Australasian Masonry Conference*. February, 11-14, Sydney, Australia.

Cattari, S., Degli Abbati, S., Ottonelli, D., Marano, C., Camata, G., Spacone, E., Da Porto, F., Modena, C., Lorenzoni, F., Magenes, G., Penna, A., Graziotti, F., Ceravolo, R., Miraglia, G., Lenticchia, E., Fiorini, N., Spina, D., 2019. Discussion on data recorded by the Italian structural seismic monitoring network on three masonry structures hit by the 2016-2017 central Italy earthquake. *COMPDYN 2019.* June 24-26, Crete, Greece.

Dolce, M., Nicoletti, M., De Sortis, A., Marchesini, S., Spina, D., Talanas, F., 2017. Osservatorio sismico delle strutture: the Italian structural seismic monitoring network. *Bulletin of Earthquake Engineering*, **15**(2), 621-641.

Graziotti, F., Toninelli, P., Solenghi, M., Guerrini, G., Penna, A., 2019. Numerical simulation of the nonlinear earthquake response of a monitored URM school building. *COMPDYN 2019.* June 24-26, Crete, Greece.

Kallioras, S., Guerrini, G., Tomassetti, U., Marchesi, B., Penna, A., Graziotti, F., Magenes, G., 2018. Experimental seismic performance of a full-scale unreinforced clay-masonry building with flexible timber diaphragms. *Engineering Structures*, 161, 231-249.

Lagomarsino, S., Penna, A., Galasco, A., Cattari, S., 2013. TREMURI program: an equivalent frame model for the nonlinear seismic analysis of masonry buildings. *Engineering Structures*, **56**, 1787-1799.

Magenes, G., Penna, A., Senaldi, I. E., Rota, M., Galasco, A., 2014. Shaking table test of a strengthened full-scale stone masonry building with flexible diaphragms. International Journal of Architectural Heritage, 8(3), 349-375.

MIT, Italian Building Code, 2008. *DM 14.01*.2008: *Norme Tecniche per le Costruzioni.* Italian Ministry of Infrastructures and Transportation, Rome.

MIT, Italian Building Code, Commentary, 2009. *Circ. 617 02.02. 2009: Istruzione per l'applicazione delle nuove Norme Tecniche per le Costruzioni.* Italian Ministry of Infrastructures and Transportation, Rome.

Penna, A., Lagomarsino, S., Galasco A., 2014. A non-linear macroelement model for the seismic analysis of masonry buildings. *Earthquake Engineering & Structural Dynamics*, **44**, 159-179.